Tilt and Rotational Pitch Angle of Membrane-Inserted Polypeptides from Combined ^{15}N and ^{2}H Solid-State NMR Spectroscopy†

Christopher Aisenbrey‡,§ and Burkhard Bechinger*,‡,§

Faculté de Chimie, Institut le Bel, Université Louis Pasteur/CNRS FRE2446, 4, rue Blaise Pascal, 67070 Strasbourg, France, and Max-Planck-Institut für Biochemie, Am Klopferspitz 18A, 82152 Martinsried, Germany

Received March 26, 2004; Revised Manuscript Received June 8, 2004

ABSTRACT: Knowledge of the alignment of α-helical polypeptides with respect to the membrane surface and their dynamics in the membrane are key to understanding the functional mechanisms of channels, antibiotics, and signal or translocation peptides. In this paper polypeptides have been labeled with [3,3,3-$^{2}H_3$]alanine as well as with ^{15}N at single site amide positions and reconstituted into oriented phospholipid bilayers. A transmembrane and two amphipathic helical polypeptides with the deuterium label at orthogonal positions have been investigated by deuterium and proton-decoupled ^{15}N solid-state NMR spectroscopy. The ^{15}N chemical shift measurements and the deuterium quadrupole splitting exhibit a highly complementary functional dependence with respect to the spatial alignment of the polypeptide. Therefore, the combination of these two measurements allows one to determine both the tilt and the rotational pitch angle with high precision. In addition, the deuterium line shape is very sensitive to mosaic spread and the relative orientation of the peptide. The solid-state NMR measurements indicate that the model sequences exhibit a small degree of mosaicity, when at the same time the phospholipid headgroup region is significantly distorted. Furthermore, the ^{2}H solid-state NMR spectra reveal small orientational and dynamic differences when the fatty acyl chain composition of the phosphatidylcholine bilayers is modified.

The structural investigation of membrane-associated proteins remains a difficult task although the subject attracts increasing interest and a limited number of high-resolution structures are deposited each year (e.g., refs *1*−*7*). On one hand, diffraction techniques and solution state NMR[1] spectroscopy are well-established methods to describe at atomic resolution the intrinsic structure of biomolecules. However, these techniques require either the availability of crystalline samples (*1*−*5*) or fast isotropic reorientation (*6*), which for most protein−membrane complexes has so far proven impossible to achieve (*7*). On the other hand, solid-state NMR spectroscopy is an emerging technique for the structural analysis of biomolecules (*8*). The method has been designed to study immobilized samples such as peptides and proteins, which are strongly associated with extended lipid bilayers (reviewed, e.g., in refs *9*−*13*).

When membrane polypeptides are investigated by solid-state NMR spectroscopy, either magic angle sample spinning is applied or static oriented samples are prepared. By these approaches accurate distance or angular information within large protein−lipid complexes has been obtained (e.g., refs *14* and *15*). Using static oriented samples the complete structure of gramicidin A, a membrane-inserted peptide, has been determined (*9*). Furthermore, proton-decoupled ^{15}N solid-state NMR spectroscopy has been shown to be particularly useful in providing detailed information on the topology of polypeptides with respect to the normal of the membrane (*16*). This piece of information is of utmost importance to our understanding of the function of membrane polypeptides (*17*, *18*).

In particular, the orientation-dependent ^{15}N chemical shift exhibits a direct functional relationship with the alignment of the main axis of α-helical polypeptides (*16*). The ^{15}N chemical shift tensor, which describes the anisotropic interactions of the ^{15}N nucleus with the magnetic field, exhibits a combination of favorable properties which combine in such a manner to allow for the evaluation of the approximate helix tilt angle solely from ^{15}N chemical shift measurements. Not only does the unique σ_{33} component of the ^{15}N chemical shift tensor exhibit an alignment close to parallel to the long axis of α-helical polypeptides but the σ_{11} and σ_{22} components are also characterized by approximately identical values. This, to first approximation, results in a line shape resembling a symmetric interaction tensor (*16*).

† We are grateful to the Agence Nationale pour la Recherche contre le SIDA for financial support, in particular for financing a Ph.D. grant to C.A.

* Corresponding author. Present address: Faculté de Chimie, Institut le Bel, 4, rue Blaise Pascal, 67070 Strasbourg, France. Tel: +33 3 90 24 51 50. Fax: +33 3 90 24 51 51. E-mail: bechinger@chimie.u-strasbg.fr.

‡ Max-Planck-Institut für Biochemie.

§ Université Louis Pasteur/CNRS FRE2446.

[1] Abbreviations: NMR, nuclear magnetic resonance; DMPC, 1,2-dimyristoyl-*sn*-glycero-3-phosphatidylcholine; DOPC, 1,2-dioleoyl-*sn*-glycero-3-phosphatidylcholine; hΦ19W, KKKALLALLALAWALALLALLALLAKKK with A = [3,3,3-$^{2}H_3$]alanine and L = [^{15}N]leucine; KL14, KKLLKKAKKLLKKL; KL15, KKLLKALKKLLKKLK; PC20:1, 1,2-eicosenoyl-*sn*-glycero-3-phosphatidylcholine (11-*cis*); POPC, 1-palmitoyl-2-oleoyl-*sn*-glycero-3-phosphatidylcholine.

10.1021/bi049409h CCC: $27.50
Published on Web 07/24/2004

Although these properties make the ^{15}N chemical shift a good indicator of the helical tilt angle (*16*), the measurements remain rather insensitive to rotation of the peptide around the helix axis (*19*). When ^{15}N-labeled peptides are investigated by proton-decoupled ^{15}N solid-state NMR spectroscopy, this rotational orientation can only be deduced by testing a number of different ^{15}N labels along the polypeptide chain (*20*, *21*). Therefore, in previous investigations several peptides each labeled at a single site have been prepared from a given sequence (*20*, *21*). Furthermore, both the orientation-dependent ^{15}N chemical shifts and the corresponding ^{1}H$-^{15}$N dipolar coupling can be extracted from separated local field spectra, analyzed, and used for structural analysis (*9*, *22*, *23*). Although this approach has also been applied to perlabeled samples, it still requires knowledge of the secondary structure preferences, the local dynamics at each site, and the unambiguous assignment of a few resonances (*10*, *16*, *23*, *24*).

Whereas the rotation angle around the helix long axis (rotational pitch angle) seems irrelevant for transmembrane helical polypeptides that exhibit fast rotational diffusion around the membrane normal, this information is of particular interest for peptides that are oriented along the membrane surface. At this interfacial location the local chemical environment changes within a few angstroms, and the rotational pitch angle thus places the individual peptide residues in their appropriate surrounding. Unfortunately, in case of in-plane oriented polypeptides the information on the rotational pitch is accurate only in exceptional cases when ^{15}N labeling alone is used (e.g., ref *25*). In addition, peptides oriented along the membrane surface exhibit exchange equilibria involving the adjacent aqueous phase (*26*, *27*). Therefore, these samples are characterized by considerable motional flexibility, which complicates the quantitative analysis of chemical shift measurements from oriented solid-state NMR spectra. Furthermore, motional averaging reduces the dipolar transfer of magnetization from ^{1}H to ^{15}N with detrimental effects on the inherently low signal-to-noise ratio observed for the ^{15}N nucleus. Additional information from other nuclei is therefore desired.

Deuterium solid-state NMR spectroscopy of ^{2}H-labeled sites provides alternative approaches (*28*, *29*). The deuterium nucleus has been used to investigate membrane-associated lipids (e.g., refs *29*−*32*), polypeptides (*33*−*38*), or water (*39*−*41*). Furthermore, oriented ^{2}H NMR spectroscopy has made important contributions during the structure determination of gramicidin A (*9*, *42*, *43*) or the retinal moiety in rhodopsin (*44*). However, the technique has, to our knowledge, so far not been explored in a systematic manner for the investigation of membrane alignments of α-helical polypeptides. Oriented deuterium solid-state NMR spectroscopy has also been applied during investigations of the effects of hydrophobic mismatch on peptide alignment (*45*) or when peptides associated with magnetically aligned bicelles were investigated (*46*−*48*). In this paper the applicability of oriented deuterium solid-state NMR spectroscopy alone and in combination with ^{15}N chemical shift data has been tested. It will be shown that important topological information is obtained for amphipathic or hydrophobic α-helical peptides using oriented ^{2}H solid-state NMR spectroscopy of deuterated alanines.

The deuterated alanine methyl group offers several distinct advantages during the solid-state NMR investigation of membrane-associated polypeptides. First, the methyl group is directly attached to the peptide backbone where the $C_\alpha-C_\beta$ bond exhibits a well-defined orientation with respect to the helix axis. Thus the alignment of this vector is related to the orientation of the helix backbone in a direct manner. Second, the methyl group carries three equivalent deuterons that are in fast exchange at ambient temperatures (*49*). The superposition of signal intensities from three sites significantly increases the sensitivity of the ^{2}H NMR measurement. Third, the alignments within the peptide structure of the $C_\alpha-C_\beta{}^{2}H_3$ vector and the unique static element σ_{33} of the ^{15}N chemical shift tensor (i.e., the helix axis) are sufficiently different, and therefore, these two measurements provide highly complementary information (*19*). Fourth, the overall deuterium signal intensity is less affected by motion when compared to the ^{15}N signal of the peptide bond obtained by cross-polarization techniques. The latter relies on signal enhancement by magnetization transfer from the abundant high-γ ^{1}H pool to the dilute ^{15}N nuclei using cross-polarization (*50*). When dipolar interactions between these nuclei are averaged by motions, the ^{15}N signal intensity is reduced or, in the limit of fast isotropic motions, even absent. In contrast, the total intensity of the deuterium NMR signal is only affected by the local and global dynamics of the peptide inasmuch as these have an influence on ^{2}H relaxation. The magnetization decay of spin ≥ 1 nuclei is largely dominated by quadrupolar interactions (*51*, *52*). Nevertheless, the deuterium line shape remains sensitive to exchange processes between different conformational and/or topological states (*28*, *29*, *38*).

In the work presented in this paper, several peptides labeled with $^{2}H_3C_\beta$-alanine were prepared, reconstituted into oriented lipid membranes, and investigated by ^{2}H solid-state NMR spectroscopy. The data provide structural as well as dynamic information on the polypeptides in oriented bilayer environments. Importantly, it will be shown that the angular restraints obtained from ^{2}H solid-state NMR spectroscopy are highly complementary to those deduced from proton-decoupled ^{15}N solid-state NMR spectra.

THEORY

The methyl group of alanine exhibits fast rotational motions around the $C_\alpha-C_\beta$ bond. As a result the ^{2}H tensor is axially symmetric with respect to the $C_\alpha-C_\beta$ bond vector. In the absence of further motional effects the measured splitting $\Delta\nu_Q$ is directly related to the orientation of the $C_\alpha-C_\beta$ bond:

$$\Delta\nu_Q = \frac{3}{2}\left(\frac{e^2qQ}{h}\right)\left(\frac{3\cos^2\Theta - 1}{2}\right) \qquad (1)$$

Here Θ is the angle between the $C_\alpha-C_\beta$ bond and the magnetic field direction and e^2qQ/h is the static quadrupolar coupling constant (*28*). Notably, C_α is an integral part of the polypeptide backbone. As a consequence, the orientation of the $C_\alpha-C_\beta$ bond also reflects the overall alignment of the peptide.

Due to rotational diffusion of the lipids and peptides in liquid crystalline membranes, the $C_\alpha-C_\beta$ bond moves on a cone of semiangle φ relative to the membrane normal. In

case of alignments of the membrane normal parallel to the magnetic field direction, the angle φ does not change during rotational diffusion; thus φ and Θ coincide. However, if other membrane alignments are studied, rotational diffusion of membrane constituents results in further averaging. With β being the angle between the membrane normal and the magnetic field direction, the averaged quadrupolar splitting is given by

$$\Delta\nu_Q = \frac{3}{2}\left(\frac{e^2qQ}{h}\right)\left(\frac{3\cos^2\varphi - 1}{2}\right)\left(\frac{3\cos^2\beta - 1}{2}\right) \quad (2)$$

For membranes oriented with the bilayer normal perpendicular to the magnetic field direction ($\beta = 90°$), the measured deuterium quadrupole splitting is thus half of the value at $\beta = 0°$. When the peptide is reconstituted into nonoriented membranes, "powder pattern spectra" are observed, where the deuterium quadrupole spectrum is characterized by two maxima at the frequencies of the $\beta = 90°$ orientation (*28*). Thus the angle φ between the $C-C^2H_3$ vector and the membrane normal can also be determined from the observed splitting of nonoriented samples when fast rotational reorientation occurs. Additional motions of the peptide relative to the membrane normal, such as for example wobbling, can be taken into consideration by replacing $(3\ \overline{\cos^2}\ \varphi - 1)/2$ by the corresponding order parameter $(3\ \overline{\cos^2\varphi} - 1)/2$, where the bar indicates the time average.

MATERIALS AND METHODS

Phospholipids were purchased from Avanti Polar Lipids (Birmingham, AL). Peptides KL14 (KKLLKKAKKLLKKL), KL15 (KKLLKALKKLLKKLK), and hΦ19W (KKKALLALLALAWALALLALLAKKK) were synthesized by solid-phase peptide synthesis on a Millipore 9060 automatic peptide synthesizer using Fmoc (9-flourenylmethyloxycarbonyl) chemistry. At the underlined positions the ^{15}N-labeled analogue of leucine or the 3,3,3-$^2H_3$-labeled analogue of alanine are incorporated. The synthetic products were purified using reversed-phase high-performance liquid chromatography. The identity of the products was confirmed by MALDI mass spectrometry.

Sample Preparation. Ten milligrams of peptide and 200 mg of lipid were codissolved in trifluoroethanol (TFE). The mixtures were applied onto 30 ultrathin cover glasses (9 × 22 mm; Paul Marienfeld GmbH & Co. KG, Lauda-Königshofen, Germany), first dried in air and thereafter in high vacuum overnight. After the samples have been equilibrated at 93% relative humidity, the glass plates were stacked on top of each other. The stacks were stabilized and sealed with Teflon tape and plastic wrappings.

NMR Measurements. Solid-state NMR spectra were recorded on a Bruker Avance wide-bore NMR spectrometer operating at 9.4 T. A commercial double-resonance solid-state NMR probe modified with flattened coils of dimensions 15 × 4 × 9 mm was used. The spectra of samples rotated by 90° relative to the magnetic field directions were acquired using a second coil of similar geometry. Proton-decoupled ^{15}N solid-state NMR spectra were acquired using cross-polarization (*50*). Typical acquisition parameters were the following: spin lock time 1.6 ms, recycle delay 3 s, ^1H B_1 field 31 kHz, 256 data points, 20000 acquisitions, and spectral width 40 kHz. Before Fourier transformation an exponential apodization function corresponding to a line broadening of 300 Hz was applied. NH_4Cl (41.5 ppm) was used as a reference corresponding to approximately 0 ppm for liquid NH_3.

Deuterium solid-state NMR spectra were recorded using a quadrupolar echo pulse sequence (*53*) with the following parameters: ^2H B_1 field 36 kHz, interpulse delay 50 μs, spectral width 100 kHz, 4096 data points, 20000 scans, and repetition time 1.5 s. The spectra were referenced relative to ^2H_2O (0 ppm). An exponential apodization function corresponding to a line broadening of 300 Hz was applied before Fourier transformation.

Proton-decoupled ^{31}P solid-state NMR spectra were recorded using a Hahn echo pulse sequence (*54*) with the following parameters: ^1H B_1 field 31 kHz, 90° pulse length 2 μs, echo delay 40 μs, spectral width 40 kHz, 512 data points, 128 scans, and repetition time 3 s. The spectra were referenced relative to 85% phosphoric acid (0 ppm). An exponential apodization function corresponding to a line broadening of 50 Hz was applied before Fourier transformation.

Calculation of Orientational Restraints from Experimental Spectra. To evaluate the peptide orientations that agree with the experimental spectra, a Cartesian coordinate system was defined in the following manner. The long axis of the α-helix defines the *z*-axis, and the *x*-axis resides within the plane dividing hydrophobic and hydrophilic sections of amphipathic helices such as KL14. Ideal α-helix conformations were assumed for analysis of peptide topology. Within the resulting reference frame the coordinates of the labeled ^{15}N atom, the corresponding amide proton, and the C atoms were extracted using the computer program Insight II (BIOSYM; Molecular Simulations, San Diego, CA).

The coordinates of the alanine C_α and the C_β atoms were needed to simulate the deuterium NMR spectra. Coordinates of the respective peptide bond were also used to calculate the ^{15}N chemical shift tensor in the same reference frame using information on ^{15}N chemical shift tensors reported in the literature (*24*). The ^{15}N chemical shift main tensor elements exhibit values of 223, 75, and 61 ppm. By successively rotating the peptide molecule around the *z*- and the *y*-axis (50 × 50 steps) the three-dimensional orientational space was systematically screened (Figure 4C). For each peptide alignment the ^{15}N chemical shift and $\Delta\nu_Q$ were calculated assuming a magnetic field direction parallel to the original *z*-axis. Contour plots mark the angular pairs that agree with the experimental results.

Simulation of the Mosaic Spread. To study the effect of orientational mosaic spread on the spectral line shape, the peak splitting is calculated for all angles Θ describing the alignment of the $C_\alpha-C_\beta$ bond relative to the magnetic field direction. In parallel, a Gaussian weighting factor, which is a function of Θ and the standard deviation σ, is calculated according to

$$\chi = \frac{1}{\sigma\sqrt{2\pi}}\exp\left(-\frac{(\Theta - \Theta_0)^2}{2\sigma^2}\right) \quad (3)$$

Thereafter, the spectra for all angles Θ are added under consideration of χ and the scaling function that results from

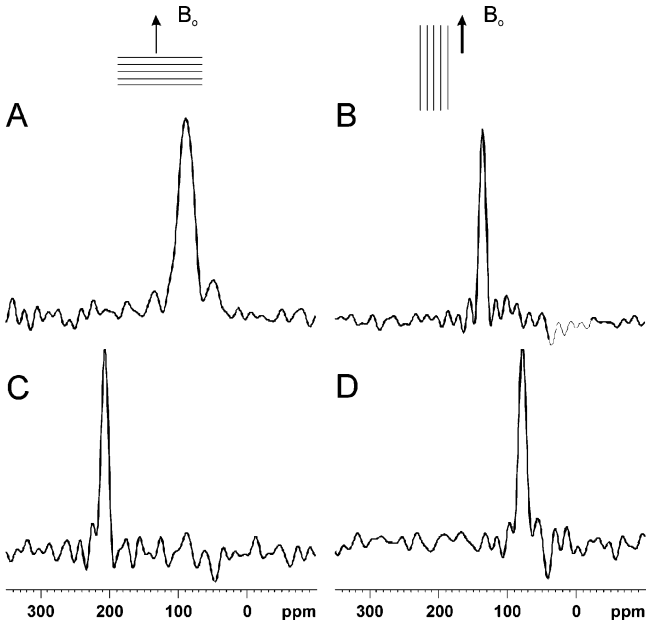

FIGURE 1: Proton-decoupled ^{15}N solid-state NMR spectra of ([3,3,3-$^{2}H_3$]alanine-7,[^{15}N]leucine-10)-KL14 (A, B) and of ([3,3,3-$^{2}H_3$]-alanine-14,[^{15}N]leucine-15)-hΦ19W (C, D) when reconstituted into oriented DOPC membranes. Spectra A and C are obtained when the membrane normal is oriented parallel to the magnetic field direction and spectra B and D when the sample is tilted by 90°.

Table 1: ^{2}H Quadrupolar Splitting and ^{15}N Chemical Shift Obtained from Solid-State NMR Spectra of Amphipathic Peptides ([3,3,3-$^{2}H_3$]alanine-7,[^{15}N]leucine-10)-KL14 and ([3,3,3-$^{2}H_3$]alanine-6,[^{15}N]leucine-7)-KL15 When Inserted into Oriented Phosphatidylcholine Bilayers[a]

	peptide							
	KL14				KL15			
lipid	^{2}H(‖) (kHz)	^{2}H(⊥) (kHz)	^{15}N(‖) (ppm)	^{15}N(⊥) (ppm)	^{2}H(‖) (kHz)	^{2}H(⊥) (kHz)	^{15}N(‖) (ppm)	^{15}N(⊥) (ppm)
POPC	15.4	8.1	87.0	136.0	6.0	2.2	74.0	144.0
DMPC	16.1	7.8	74.5	143.4	7.6	3.9	73.3	144.0
PC20:1	16.4	8.2	74.0	145.0	8.3	4.2	73.2	144.0
DOPC	17.4	8.4	85.8	137.0	10.8	4.9	74.0	144.0

[a] The values are given for sample orientations with the bilayer normal parallel (‖) or perpendicular (⊥) to the magnetic field direction.

integration of polar coordinates. This last step was repeated in a recursive manner until the distance between the intensity maxima of the calculated spectrum agrees with that of the experimental line shape.

RESULTS

α-Helical peptides were synthesized and labeled with [$^{2}H_3$]-alanine as well as [^{15}N]leucine, reconstituted into oriented phospholipid bilayers, and investigated by solid-state NMR spectroscopy. Proton-decoupled ^{15}N solid-state NMR spectra of KL14 labeled with [^{15}N]leucine-10 and [3,3,3-$^{2}H_3$]alanine-7 exhibit ^{15}N chemical shifts of 86 ppm when investigated in DOPC bilayers (Figure 1A, Table 1). ^{15}N chemical shifts values <100 ppm are indicative of peptide alignments parallel to the membrane surface (*16*). The ^{2}H NMR spectrum of the same sample is shown in Figure 2A. A single well-resolved quadrupolar spitting of 17.4 kHz is observed at room temperature, indicative of fast rotational averaging around the $C_\alpha-C_\beta$ bond. This motion ensures fast exchange of the positions of the methyl deuterons and results in a single quadrupolar splitting for all three labeled sites. Furthermore, the "oriented" spectral line shape shows that the peptide is well aligned with respect to the magnetic field direction. In the central region of the spectrum another signal with narrow splitting appears, which arises at least in part from water deuterons (natural abundance 0.015%). Due to the interactions of these water molecules with the membrane surfaces, this signal also reveals a small degree of ordering (*39*−*41*).

When a related peptide, ([$^{2}H_3$]alanine-6,[^{15}N]leucine-7)-KL15, is reconstituted in DOPC the experimentally observed quadrupolar spitting is 10.8 kHz (Table 1). The ^{15}N chemical shift of the same sample occurs at 74 ppm (Table 1), indicative of peptide orientations approximately parallel to the membrane surface (*16*). Peptides KL14 and KL15 were designed using helical wheel analysis, and the position of the alanine residue was chosen to be different by 80° relative to the hydrophobic−hydrophilic interface (Figure 3). Differences in the experimental quadrupolar splittings thus reflect the different alignment of the $C_\alpha-C_\beta$ bond vector relative to the membrane normal (cf. Theory section).

When the samples are rotated by 90° well-resolved peak pairs are again observed in deuterium and proton-decoupled ^{15}N solid-state NMR spectra (Figures 1B and 2B). A ^{15}N chemical shift value of 137 ppm is observed. In this configuration the orientation of the helix axis can be parallel or perpendicular to the magnetic field direction, which results in ^{15}N chemical shifts close to σ_{33} (>200 ppm) or σ_{11}/σ_{22} (<100 ppm), respectively (*55*). The observed value between these extremes thus indicates fast motional averaging around the membrane normal.

The deuterium quadrupole splittings exhibit values of 8.4 and 4.9 kHz for KL14 and KL15, respectively (Table 1). Within experimental error these measurements correspond to half the values observed when oriented with the membrane normal parallel to the magnetic field direction. Therefore, at room temperature these short peptides exhibit fast rotational diffusion around the membrane normal concomitant with efficient averaging of the ^{15}N chemical shift as well as the ^{2}H NMR time scales.

The α-helical sequence hΦ19W is composed of alternating alanine and leucine residues interrupted by tryptophan at position 13 (*56*). Three lysines flank each terminus, and isotopic labels are incorporated at positions 14 ([$^{2}H_3$]alanine) and 15 ([^{15}N]leucine). The proton-decoupled ^{15}N solid-state NMR spectrum of hΦ19W reconstituted into oriented DOPC membranes exhibits a sharp peak at 205 ppm indicating a transmembrane orientation (Figure 1C). The deuterium spectrum shows a well-defined splitting of 16.3 kHz (Figure 2D). When the sample is rotated by 90°, the ^{15}N resonance moves to 76 ppm (Figure 1D), and at the same time the deuterium quadrupole splitting reduces to 7.7 kHz (Figure 2E). In addition, this figure reveals a low-intensity contribution with ^{2}H quadrupolar splittings of about 24 kHz. This signal intensity is less apparent at alignments of the membrane normal parallel to the magnetic field direction due to partial overlap with the main peaks (Figure 2D).

Notably, the quadrupolar splittings observed at ambient temperature in the ^{2}H solid-state NMR spectra of the hydrated membrane powders (Figure 2C,F) correspond to the peak-to-peak distances observed at 90° orientations of the oriented samples (Figure 2B,E). In contrast, at 263 K the ^{2}H NMR

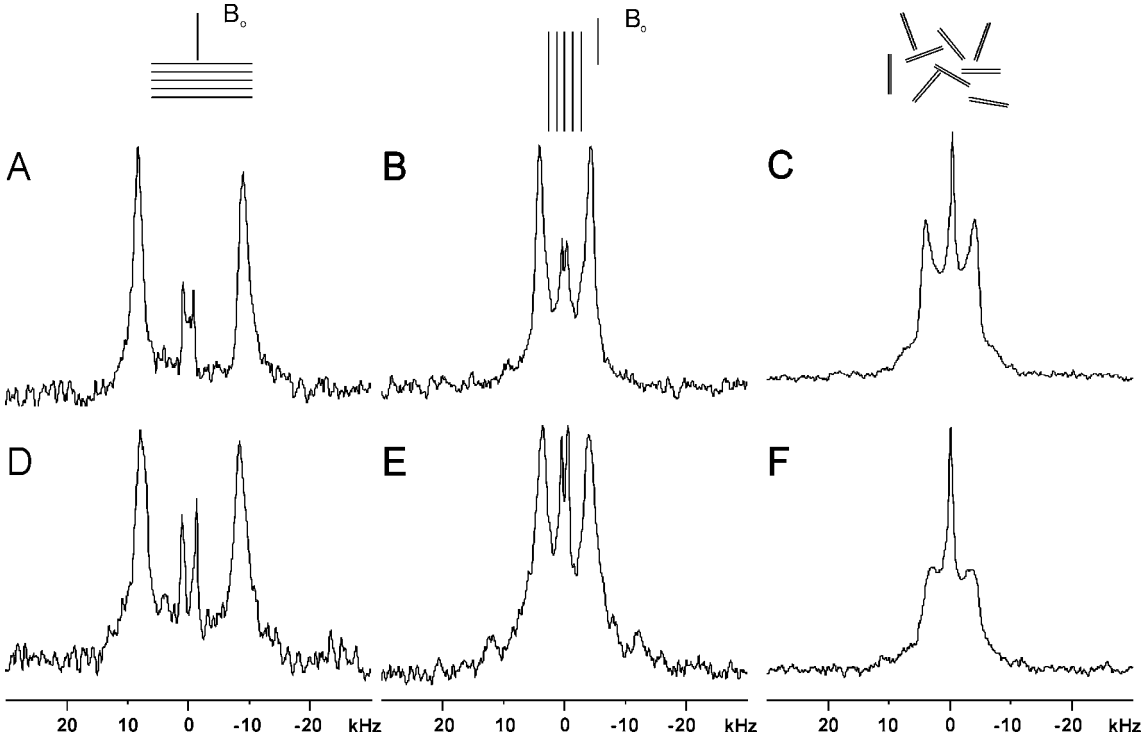

FIGURE 2: Deuterium solid-state NMR spectra of ([3,3,3-$^2H_3$]alanine-7,[^{15}N]leucine-10)-KL14 (A−C) and of ([3,3,3-$^2H_3$]alanine-14,[^{15}N]-leucine-15)-hΦ19W (D−F) when reconstituted into DOPC membranes. Spectra A and D are obtained after the peptides were reconstituted into oriented membranes with the normal aligned parallel to the magnetic field direction, spectra B and E after the samples were tilted by 90°, and spectra C and F from nonoriented bilayers.

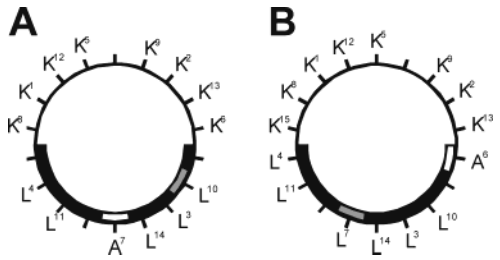

FIGURE 3: Edmundson helical wheel diagrams of KL14 and KL15. The positions of the labeled amino acid carrying the ^{15}N and ^{2}H nuclei are marked in gray and white, respectively.

spectrum of hΦ19W reconstituted in hydrated, nonoriented DMPC paste exhibits a powder pattern line shape exhibiting ^{2}H quadrupolar splittings of 38 kHz (not shown). This latter result indicates that fast rotation around the $C_\alpha-C_\beta$ bond continues although efficient molecular diffusion is abolished (*49*).

Although neither the deuterium quadrupole splitting nor the ^{15}N chemical shift defines the alignment of the peptide helix in an unambiguous manner, they provide restraints to reduce the number of possible orientations. Figure 4A represents the spatial alignments of KL14 that agree with the measured ^{15}N chemical shift and ^{2}H quadrupolar splitting. To this effect a helical peptide model has been placed in the reference coordinate system, where initially the *z*-axis is oriented parallel to the helix axis and the $x-y$ plane separates the hydrophobic from the hydrophilic part of the amphipathic polypeptide (Figure 4C). The peptide was successively rotated around two angles perpendicular to each other. For each alignment the resulting values of ^{15}N chemical shift and ^{2}H quadrupolar splitting were calculated. The contours shown in Figure 4A indicate those orientations that agree with the experimental chemical shift of the ^{15}N resonance (dashed line) or with the measured ^{2}H quadrupolar splitting (solid line) at sample alignments with the normal parallel to the magnetic field direction. Potential errors are taken into account by additional contours, which result when the experimental values deviate by ±5 ppm or ±1 kHz, respectively.

Six peptide alignments agree with both the deuterium and the ^{15}N NMR measurements (Figure 4). Figure 4B shows models of perfect α-helical structure, which were located within an interface at orientations that correspond to the calculated angular pairs. Some of the calculated orientations shown are associated with a deep insertion into the membrane interior of lysine side chains and are, therefore, excluded. On the other hand, the lysines are well exposed to the water phase when at the same time the leucines are located within the membrane interior for the angular pairs that correspond to intersection VI of the contour plot.

To investigate the effect of the lipid composition on helix alignment, KL14 and KL15 were reconstituted into phosphatidylcholine membranes of different fatty acyl chain composition. Table 1 provides the ^{15}N chemical shift values and the deuterium quadrupolar splittings, $\Delta\nu_Q$, of KL14 and KL15 when reconstituted into four different phospholipids. The deuterium quadrupolar splitting of KL14 is 15.4 kHz when reconstituted into POPC membranes and increases in the presence of DMPC (16.1 kHz), PC20:1 (16.4 kHz), and DOPC (17.4 kHz). The same order is observed for KL15, where $\Delta\nu_Q$ varies between 6.0 kHz (POPC) and 10.8 kHz (DOPC). Comparison of $\Delta\nu_Q$ obtained in different lipid environments thus reveals significant differences. In contrast, the ^{15}N chemical shift value measured for [^{15}N]leucine-7 of KL15 is independent of the bilayer lipid used (Table 1). The ^{15}N chemical shift of [^{15}N]leucine-10 of KL14 is similar

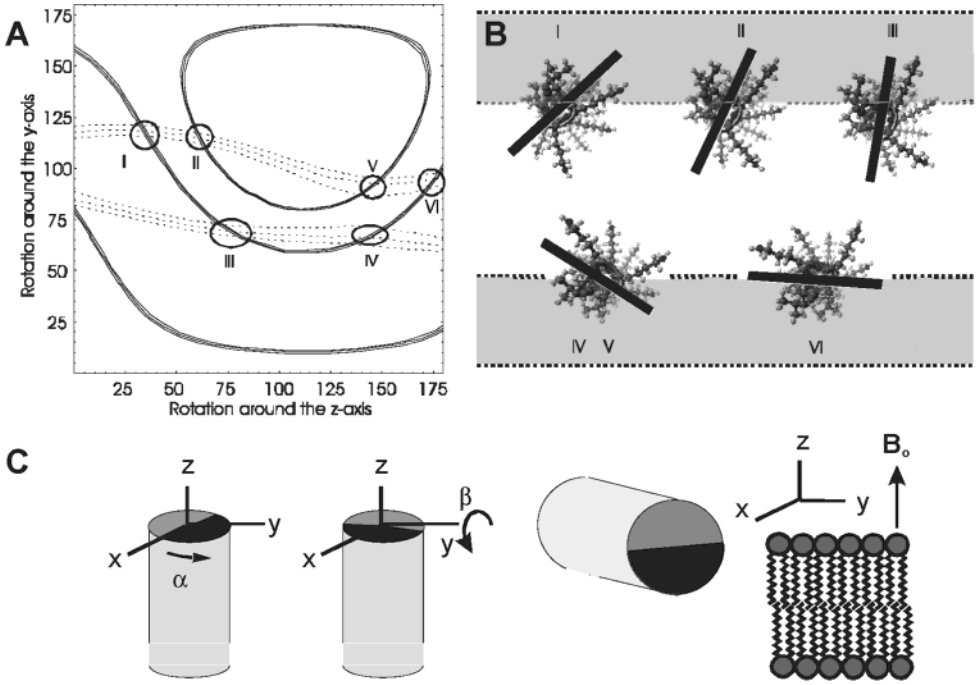

FIGURE 4: Possible alignments of ([3,3,3-$^{2}H_3$]alanine-7,[^{15}N]leucine-10)-KL14 reconstituted in oriented DOPC bilayers calculated from the ^{2}H quadrupolar splitting and the ^{15}N chemical shift information obtained from alignments of the sample normal parallel to the magnetic field direction (cf. text for details). In panel A the possible spatial orientations of the peptide are represented by the helical tilt and the rotational pitch angles. The solid lines trace angular pairs that agree with the experimental ^{2}H quadrupolar splitting of 17.4 ± 1 kHz, and the dotted lines are in agreement with the ^{15}N chemical shift of 85 ±5 ppm. The cross sections are labeled, and the corresponding peptide orientations relative to the membrane interface are shown in panel B. Whereas the gray shading in panel B represents the hydrophobic membrane interior, the white regions correspond to the hydrophilic regions of the interface and water. (C) The successive rotations of the helix around the helix long axis (*z*-direction) and an axis perpendicular to that (*y*-direction) are illustrated (cf. text for details).

when reconstituted in POPC (87 ppm) or DOPC membranes (86 ppm). However, these values are significantly different when compared to those obtained in the presence of DMPC (75 ppm) or PC20:1 (74 ppm). These results are confirmed when proton-decoupled ^{15}N spectra are recorded from KL14 samples tilted by 90°. The measured ^{15}N chemical shifts are 143−145 ppm in the presence of DMPC or PC20 and 136−137 ppm for POPC and DOPC membranes.

The deuterium solid-state NMR spectra of KL14, KL15, and hΦ19W show well-resolved peaks (Figure 2), suggesting that the peptides exhibit a homogeneous orientation with respect to the magnetic field direction. In contrast, other samples investigated by us exhibit broad deuterium NMR line shapes, suggesting a heterogeneous distribution of peptide alignments even when ^{31}P NMR spectroscopy indicates that the lipids are well aligned (manuscript in preparation). This observation suggests that the ^{2}H quadrupolar splitting is much more sensitive to sample mosaic spread when compared to the ^{31}P chemical shift. Therefore, we decided to investigate the effect of mosaic spread on the ^{2}H and ^{31}P solid-state NMR line shapes in more detail.

At a given average orientation of the $C_\alpha-C_\beta$ bond (i.e., 10°, 40°, 50°, or 70°) spectra were simulated with Gaussian mosaic spreads ranging from 1° to 15° (Figure 5). A close to maximal deuterium quadrupole splitting is obtained at 10° orientations of the alanine side chain. The peaks broaden asymmetrically toward smaller splitting values with increasing mosaic spread. On the other hand, at orientations near the magic angle (40° and 50°) the peaks broaden symmetrically into both directions. Already at relatively small mosaicity of about 10° (at 40° orientation) or 5° (at 50° orientation) the two ^{2}H peaks merge into a broad-frequency distribution. Yet another behavior is observed at 70° orientations. Due to the mosaic spread the peaks broaden asymmetrically, thereby effectively increasing the distance between the peak maxima. When a mosaic spread of 15° is reached, the main intensities are separated by 38 kHz, which corresponds to the peak-to-peak distance, but not the line shape, observed in powdered samples.

By comparing the experimental spectra with the line shapes of our simulations, it is evident that the model peptides KL14, Kl15, and hΦ19W exhibit a very small mosaic spread (Figures 2 and 5). In contrast, the deuterium NMR spectra of some naturally occurring amino acid sequences are characterized by broad spectral distributions of the ^{2}H NMR line shape (manuscript in preparation).

Figure 6 compares the experimental deuterium NMR spectrum of KL14 in DOPC with simulated peak intensities. Two orientations of the $C_\alpha-C_\beta$ bond are in agreement with the measured distance between peak maxima. These are an orientation of 45.31° corresponding to a positive value of $\Delta\nu_Q$ (+17.4 kHz) or an alignment of 65.46° corresponding to −17.4 kHz. To account for the spectral line shape, a mosaic spread was superimposed. Best fits were obtained when standard deviations of the Gaussian distribution of alignments of 1° are applied. An ambiguity remains, as we cannot determine the sign of $\Delta\nu_Q$ from the ^{2}H NMR spectra alone (Figure 2). However, when tilt and rotational pitch angles are calculated, the helix orientations associated with the positive quadrupolar splitting are represented by the closed contour in Figure 4A (containing intersections II and V). In contrast, peptide alignments that are associated with negative $\Delta\nu_Q$ values are represented by the open lines. Therefore, the same arguments that resulted in the selection

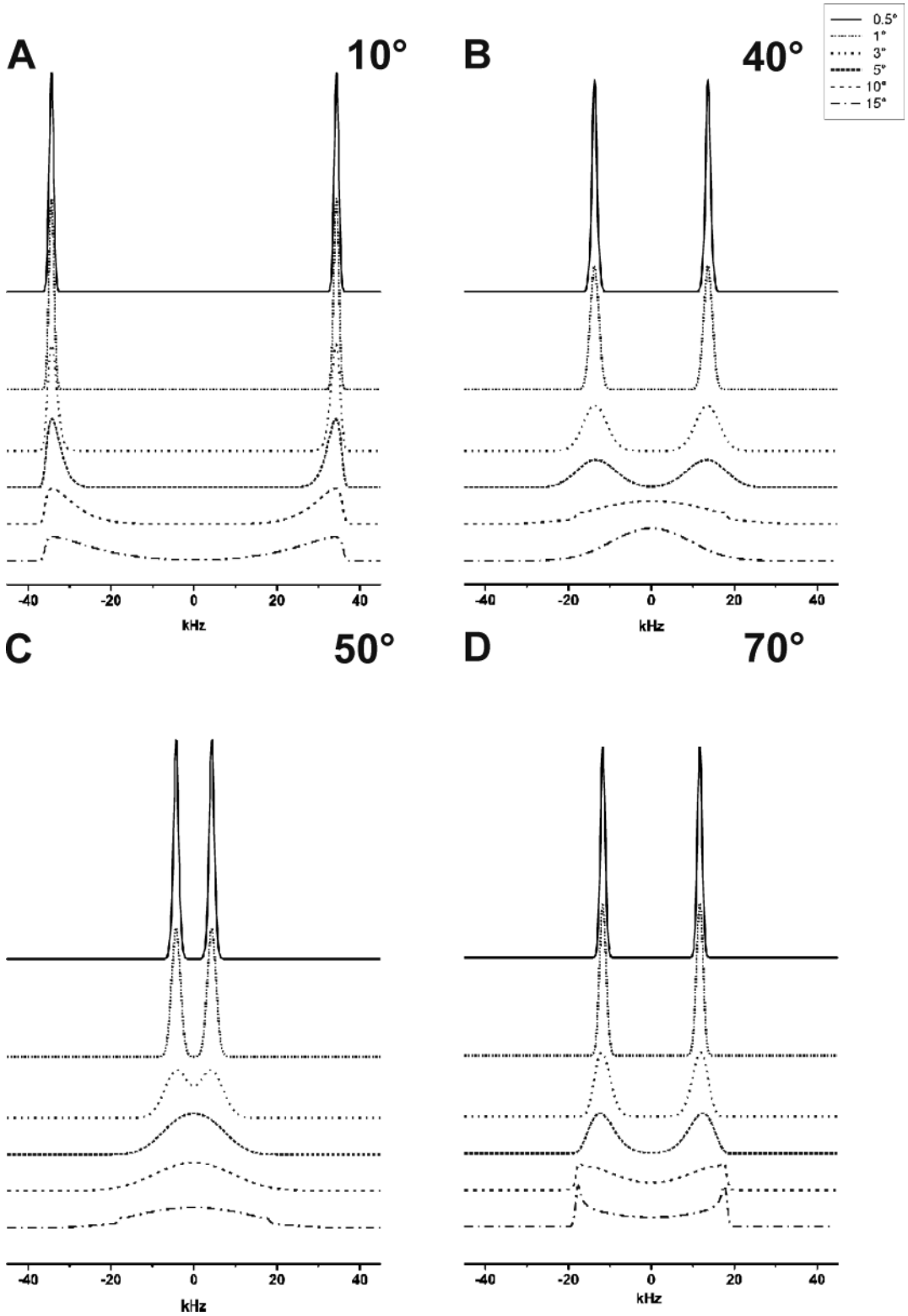

FIGURE 5: Simulated deuterium NMR spectra of [3,3,3-$^2H_3$]alanine oriented with the $C_\alpha-C_\beta$ bond at angles of 10°, 40°, 50°, or 70° relative to the magnetic field direction in the presence of a Gaussian mosaic spread of 0.5°, 1°, 3°, 5°, 10°, or 15°.

of configuration VI as being the most probable alignment also indicate that $\Delta\nu_Q$ must be −17.4 kHz.

This contrasts a mosaic spread of 6° found when the spectral line shapes of the corresponding ^{31}P solid-state NMR spectra are analyzed (Figure 7). The better orientation at the level of the peptide when compared to the lipid headgroup region suggests that the lipid bilayer, although well aligned on a macroscopic level, exhibits microscopic heterogeneity. This can be due to conformational changes of the phospholipid headgroup, for example, due to electrostatic interactions (*30*), or the molecular disordering effect of the lipid molecules as a whole (*57*) or both.

DISCUSSION

Solid-state NMR spectroscopy on oriented bilayer samples has become an established method to investigate the structure

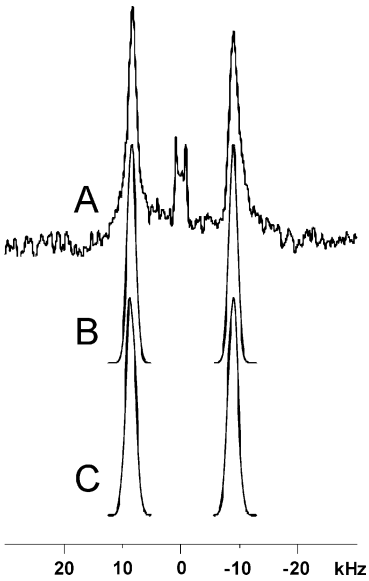

FIGURE 6: (A) Experimental ^{2}H solid-state NMR spectrum of ([3,3,3-$^{2}H_3$]alanine-7,[^{15}N]leucine-10)-KL14 when reconstituted into oriented DOPC membranes. The membrane normal is aligned parallel to the magnetic field direction. When the experimental and simulated spectra are compared to each other, good agreement in the positioning and line shape is obtained at angles of the $C_\alpha-C_\beta$ bond relative to the magnetic field vector of 45.31° (B) or 65.46° (C). In both simulations the Gaussian mosaic spread is 1°.

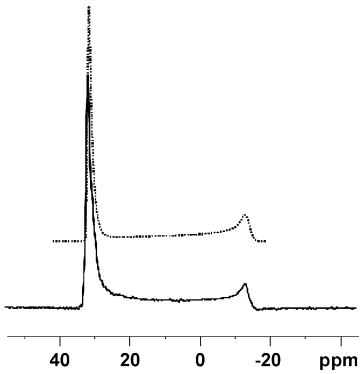

FIGURE 7: Simulation of the ^{31}P NMR experimental line shape of KL14 in DOPC phospholipid bilayers. The simulated spectrum (hatched line) was obtained by superimposing the resonance of oriented phosphatidylcholine (0° tilt angle, mosaic spread 6°) and a powder pattern line shape representing 20% of the total signal intensity.

and the orientation of membrane-associated peptides (*9*, *16*). Whereas the ^{15}N chemical shifts of peptide bonds labeled with ^{15}N alone already provide a sensitive measure of the approximate tilt angle of α-helices (*16*), more accurate information is obtained when additional orientational constraints are available (*9*). Whereas the ^{15}N chemical shift is virtually insensitive to the rotation angle around the helix long axis, the deuterium NMR quadrupole splitting of [$^{2}H_3$]-alanine-labeled peptides provides a highly complementary parameter that restricts both the tilt and the axial angles (*19*). Here we evaluate in a systematic manner the usefulness of ^{2}H solid-state NMR of alanines carrying a deuterated methyl group. The technique is tested on several model peptides labeled simultaneously with [^{15}N]leucine as well as [$^{2}H_3$]-alanine at specific sites.

The peptides were designed to orient either in a transmembrane fashion (hΦ19W) or in an alignment parallel to the membrane surface (KL14 and KL15). When monomeric, all three peptides are expected to exhibit fast rotational diffusion around the membrane normal. Proton-decoupled ^{15}N solid-state NMR spectra of hΦ19W in oriented phosphatidylcholine bilayers confirm the transmembrane alignment of the peptide. The ^{15}N labels exhibit sharp ^{15}N resonances, thereby suggesting a homogeneous alignment of the peptide relative to the magnetic field direction (Figure 1C,D). Furthermore, the deuterium solid-state NMR spectra of this peptide are characterized by well-defined pairs of resonances (Figure 2D,E). Upon closer inspection a second low-intensity ^{2}H contribution, which is characterized by a quadrupole splitting of 24 kHz, becomes apparent in the deuterium solid-state NMR spectra. This contribution is best visible at alignments of the membrane normal perpendicular to the magnetic field direction when the ^{2}H NMR signals of the principal contribution have shifted to a different spectral region (Figure 2E).

Deuterium NMR line shape analysis at sample orientations parallel as well as perpendicular to the magnetic field direction indicates that the principal signal contribution arises from peptides that undergo fast rotational diffusion. The alanine site of these peptides is well oriented relative to the magnetic field and characterized by a mosaic spread of $\leq 2°$. The broad low-intensity signals with $\Delta\nu_Q = 24$ kHz are probably due to peptide aggregates that do not rotate fast enough to fully average the deuterium quadrupolar interaction (Figure 2E).

To fully determine the membrane alignment of in-planar peptides such as KL14 and KL15, orientational restraints from deuterium solid-state NMR spectra are required to complement the ^{15}N chemical shift information. Both deuterium and ^{15}N solid-state NMR spectra indicate a homogeneous alignment of the KL14- and KL15-labeled sites. The spectra thus allow the investigation of the peptides' membrane alignment with high precision. The orientational constraints represented in Figure 4 are obtained from ^{2}H and ^{15}N solid-state NMR spectra of KL14 reconstituted in DOPC membranes. Peptide alignments that agree with both experimental measurements are found at the intersection of contours from the two measurements. However, the configurations associated with intersections labeled I−V are characterized by full or partial insertion of the lysine side chains into the membrane interior (Figure 4B). Due to the high energetic penalties of such arrangements these results are excluded from further consideration. In contrast, the alignment represented by intersection VI is characterized by favorable localizations of hydrophobic residues in the membrane interior when at the same time the lysine side chains are exposed to the aqueous environment (Figure 4B). Therefore, intersection VI represents the lowest potential energy configuration. Thus the combination of experimental data and thermodynamic considerations allows one to accurately determine the membrane orientation of the peptide. In DOPC the alignment of KL14 is characterized by a rotation around the helix long axis (*z*-axis) of 175°, this value reflecting the ideal positioning of the hydrophobic and hydrophilic residues within the membrane interface, and a tilt angle (i.e., rotation around the *y*-axis) of 95°. Figure 4A also indicates that errors in determining the chemical shifts or the quadrupolar splittings translate into deviations of about 5° in tilt and rotational pitch angles.

To determine the alignment of peptides in an absolute manner, systematic errors also have to be taken into consideration. For example, in this work we have utilized published values for the size and the orientation of the ^{15}N tensor. This is justified as the purpose of this paper is to introduce a deuterium NMR approach that allows one to gain additional insight into the topology of membrane-associated helices. Deviations from the ideal ^{15}N tensor values in real systems have to be considered if precise information about the absolute alignment of the peptides is required. How uncertainties in the definition of the ^{15}N tensor elements are translated into errors in the angular constraints is difficult to generalize. Whereas errors in σ_{33} exhibit their strongest effects when tilt angles of transmembrane peptides are determined, the analysis of helix in-plane alignments is most strongly affected by σ_{11} and σ_{22} contributions, Notably, due to the small difference between σ_{11} and σ_{22} errors, their determination can result in a large uncertainty of the rotational pitch angle. To obtain more accurate information about the absolute alignment of bonds or molecules, the averaged tensor values under exactly the same experimental conditions are required (*24*). Fortunately, complementary information obtained from deuterium solid-state NMR spectra alleviates many of these problems. Additional systematic errors arise from the assumption that the peptides adopt perfect α-helical conformations in membrane environments.

Considerable changes of the deuterium quadrupolar splitting of [$^2H_3$]alanine-labeled membrane peptides are observed when the length or the degree of saturation of the fatty acyl chains or both are modified (Table 1). At the same time the chemical composition of the phosphatidylcholine headgroup remains constant. The data presented in Table 1 indicate that peptides KL14 and KL15 are oriented parallel to the membrane surface at tilt angles close to 90°. A quantitative analysis indicates that the change in $\Delta\nu_Q$ by 4.8 kHz observed for KL15 when transferred from DOPC into POPC corresponds to a change in angle of only 2°. Clearly, this type of ^2H solid-state NMR measurement is very sensitive to small relative alterations.

Amphipathic peptides when inserted into the lipid bilayer interface have been shown to profoundly distort the packing of the membrane interior, thereby resulting in decreased order of the fatty acyl chain packing and membrane thinning (*58*−*60*). This implies that shortening the length of the fatty acyl chains decreases the total volume of the lipid hydrophobic part, which can be used to compensate for peptide-induced distortions (*17*). On the other hand, changes in the interior of the lipid bilayer exert strong effects also at the level of the membrane interface. Thus the quadrupolar splitting of deuterated water when associated with pure DOPC bilayers is 2-fold increased when compared to that of POPC membranes at the same degree of hydration (*41*). Furthermore, hydration significantly increases when peptides are inserted into the membrane (*40*). These effects can be explained by changes in lipid packing density concomitant with alterations in the area per lipid (*41*). Our data indicate that the small differences in peptide alignment and/or dynamics reflect changes in the hydrophobic interior of the membrane.

The quadrupolar splitting is strongly dependent on the angle between the $C_\alpha-C_\beta$ bond and the magnetic field. On one hand, this correlation is advantageous as it allows one to analyze peptide alignments with high precision. On the other hand, even a small mosaic spread results in considerable line broadening (Figure 5) concomitant with reduced signal-to-noise ratios. In addition, the asymmetry in line broadening prevents a simple read-out analysis of the average $\Delta\nu_Q$ by measuring the distance between the peak maxima. In these cases simulations of the spectral line shape are necessary to characterize the orientational distribution function in a reliable manner (Figure 5D).

Peptides KL14, KL15, and hΦ19W show well-resolved peaks in deuterium spectra with little mosaic spread. For other peptide sequences, especially those of natural composition, this is not always the case. We suggest that the stable and homogeneous alignment of model peptides results from their design using only a few amino acids and a clear-cut separation of hydrophobic and hydrophilic domains. In addition, the high charge density prevents aggregation, which would reduce motional averaging.

In summary, we have shown that well-oriented ^2H solid-state NMR spectra can be obtained in oriented lipid bilayers from [$^2H_3$]alanine-labeled peptides exhibiting low mosaic spread. The measured ^2H NMR quadrupole splittings are very sensitive to the orientation of the $C_\alpha-C_\beta{}^2H_3$ bond with respect to the membrane normal, thereby providing structural data highly complementary to the tilt angle information from ^{15}N chemical shift spectra. A detailed line shape analysis using spectral simulations provides valuable information of the average peptide alignment as well as the orientational mosaic spread of the labeled sites. ^2H solid-state NMR spectroscopy can thus provide a valuable source for structural analysis of membrane-associated polypeptides.

ACKNOWLEDGMENT

We acknowledge the initial help of Josefine März during peptide synthesis and purification and Monika Zobawa for recording mass spectra. We are grateful to Bas Vogt, who performed some preliminary studies on the subject.

REFERENCES

1. Buchanan, S. K. (1999) beta-Barrel proteins from bacterial outer membranes: structure, function and refolding, *Curr. Opin. Struct. Biol. 9*, 455−461.
2. Garavito, R. M. (1998) Membrane protein structures: The known world expands, *Curr. Opin. Struct. Biol. 9*, 344−349.
3. Toyoshima, C., Nakasako, M., Nomura, H., and Ogawa, H. (2000) Crystal structure of the calcium pump of sarcoplasmatic reticulum at 2.6 Å resolution, *Nature 405*, 647−654.
4. Palczewski, K., Kumasaka, T., Hori, T., Behnke, C. A., Motoshima, H., Fox, B. A., Le Trong, I., Teller, D. C., Okada, T., Stenkamp, R. E., Yamamoto, M., and Miyano, M. (2000) Crystal structure of thodopsin: A G protein-coupled receptor, *Science 289*, 739−745.
5. Striebeck, M., and Michel, H. (2004) Membrane proteins of known structure, http://www.mpibp-frankfurt.mpg.de/michel/public/memprotstruct.html.
6. Arora, A., Abildgaard, F., Bushweller, J. H., and Tamm, L. K. (2001) Structure of outer membrane protein A transmembrane domain by NMR spectroscopy, *Nat. Struct. Biol.*, 334−338.
7. Fernandez, C., Hilty, C., Bonjour, S., Adeishvili, K., Pervushin, K., and Wuthrich, K. (2001) Solution NMR studies of the integral membrane proteins OmpX and OmpA from *Escherichia coli*, *FEBS Lett. 504*, 173−178.
8. Castellani, F., van Rossum, B., Diehl, A., Schubert, M., Rehbein, K., and Oschkinat, H. (2002) Structure of a protein determined by solid-state magic-angle-spinning NMR spectroscopy, *Nature 420*, 98−102.

9. Cross, T. A. (1997) Solid-state nuclear magnetic resonance characterization of gramicidin channel structure, *Methods Enzymol. 289*, 672−696.
10. Davis, J. H., and Auger, M. (1999) Static and magic angle spinning NMR of membrane peptides and proteins, *Prog. NMR Spectrosc. 35*, 1−84.
11. Griffin, R. G. (1998) Dipolar recoupling in MAS spectra of biological solids, *Nat. Struct. Biol., NMR Suppl. 5*, 508−512.
12. Bechinger, B., Kinder, R., Helmle, M., Vogt, T. B., Harzer, U., and Schinzel, S. (1999) Peptide structural analysis by solid-state NMR spectroscopy, *Biopolymers 51*, 174−190.
13. Watts, A. (1999) NMR of drugs and ligands bound to membrane receptors, *Curr. Opin. Biotechnol. 10*, 48−53.
14. Helmle, M., Patzelt, H., Gärtner, W., Oesterhelt, D., and Bechinger, B. (2000) Refinement of the geometry of the retinal binding pocket in dark adapted bacteriorhodpsin by heteronuclear solid-state NMR distance measurements, *Biochemistry 39*, 10066−10071.
15. Jaroniec, C. P., Lansing, J. C., Tounge, B. A., Belenky, M., Herzfeld, J., and Griffin, R. G. (2001) Measurement of dipolar couplings in a uniformly (13)C,(15)N-labeled membrane protein: distances between the Schiff base and aspartic acids in the active site of bacteriorhodopsin, *J. Am. Chem. Soc. 123*, 12929−12930.
16. Bechinger, B., and Sizun, C. (2003) Alignment and structural analysis of membrane polypeptides by 15N and 31P solid-state NMR spectroscopy, *Concepts Magn. Reson. 18A*, 130−145.
17. Bechinger, B. (1999) The structure, dynamics and orientation of antimicrobial peptides in membranes by solid-state NMR spectroscopy, *Biochim. Biophys. Acta 1462*, 157−183.
18. Bechinger, B. (2001) Solid-state NMR investigations of interaction contributions that determine the alignment of helical polypeptides in biological membranes, *FEBS Lett. 504*, 161−165.
19. Bechinger, B., Aisenbrey, C., Sizun, C., and Harzer, U. (2001) ^{2}H, ^{15}N and ^{31}P solid-state NMR structural studies of polypeptides reconstituted into oriented membranes, in *The Future of Solid State NMR in Biology* (conference proceeding) (de Groot, H. J., and Kiihne, Eds.) pp 45−54, Leiden, The Netherlands.
20. Wray, V., Kinder, R., Federau, T., Henklein, P., Bechinger, B., and Schubert, U. (1999) Solution structure and orientation of the transmembrane anchor domain of the HIV-1 encoded virus protein U (Vpu) by high-resolution and solid-state NMR spectroscopy, *Biochemistry 38*, 5272−5282.
21. Kovacs, F. A., Denny, J. K., Song, Z., Quine, J. R., and Cross, T. A. (2000) Helix tilt of the M2 transmembrane peptide from influenza A virus: An intrinsic property, *J. Mol. Biol. 295*, 117−125.
22. Bechinger, B., Zasloff, M., and Opella, S. J. (1993) Structure and Orientation of the Antibiotic peptide Magainin in Membranes by Solid-State NMR Spectroscopy, *Protein Sci. 2*, 2077−2084.
23. Wang, J., Denny, J., Tian, C., Kim, S., Mo, Y., Kovacs, F., Song, Z., Nishimura, K., Gan, Z., Fu, R., Quine, J. R., and Cross, T. A. (2000) Imaging membrane protein helical wheels, *J. Magn. Reson. 144*, 162−167.
24. Teng, Q., and Cross, T. A. (1989) The in situ determination of the 15N chemical-shift tensor orientation in a polypeptide, *J. Magn. Reson. 85*, 439−447.
25. Henklein, P., Kinder, R., Schubert, U., and Bechinger, B. (2000) Membrane interactions and alignment of the structures within HIV-1 Vpu cytoplasmic domain: Effect of phosphorylation of serines 52 and 56, *FEBS Lett. 482*, 220−224.
26. Schwarz, G., Stankowski, S., and Rizzo, V. (1986) Thermodynamic analysis of incorporation and aggregation in a membrane: Application to the pore-forming peptide alamethicin, *Biochim. Biophys. Acta 861*, 141−151.
27. Montich, G., Scarlata, S., McLaughlin, S., Lehrmann, R., and Seelig, J. (1993) Thermodynamic characterization of the association of small basic peptides with membranes containing acidic lipids, *Biochim. Biophys. Acta 1146*, 17−24.
28. Seelig, J. (1977) Deuterium magnetic resonance: Theory and application to lipid membranes, *Q. Rev. Biophys. 10*, 353−418.
29. Griffin, R. G. (1981) Solid-state nuclear magnetic resonance of lipid bilayers, *Methods Enzymol. 72*, 108−173.
30. Seelig, J., Macdonald, P. M., and Scherer, P. G. (1987) Phospholipid headgroups as sensors of electric charge in membranes, *Biochemistry 26*, 7535−7541.
31. Marsan, M. P., Muller, I., Ramos, C., Rodriguez, F., Dufourc, E. J., Czaplicki, J., and Milon, A. (1999) Cholesterol orientation and dynamics in dimyristoylphosphatidylcholine bilayers: A solid-state deuterium NMR analysis, *Biophys. J. 76*, 351−359.
32. Trouard, T. P., Nevzorov, A. A., Alam, T. M., Job, C., Zajicek, J., and Brown, M. F. (1999) Influence of cholesterol on dynamics of dimyristoylphosphatidylcholine bilayers as studied by deuterium NMR relaxation, *J. Chem. Phys. 110*, 8802−8818.
33. Rothgeb, T. M., and Oldfield, E. (1981) Nuclear magnetic resonance of heme protein crystals, *J. Biol. Chem. 256*, 1432−1446.
34. Sharpe, S., and Grant, C. W. M. (2000) A transmembrane peptide from the human EGF receptor: Behaviour of the cytoplasmic juxtamembrane domain in lipid bilayer, *Biochim. Biophys. Acta 1468*, 262−272.
35. Sharpe, S., Barber, K. R., Grant, C. W., Goodyear, D., and Morrow, M. R. (2002) Organization of model helical peptides in lipid bilayers: insight into the behavior of single-span protein transmembrane domains, *Biophys. J. 83*, 345−358.
36. Pauls, K. P., MacKay, A. L., Soderman, O., Bloom, M., Tanjea, A. K., and Hodges, R. S. (1985) Dynamic properties of the backbone of an integral membrane polypeptide measured by 2H-NMR, *Eur. Biophys. J. 12*, 1−11.
37. Davis, J. H. (1988) 2H nuclear magnetic resonance of exchange-labeled gramicidin in an oriented lyotropic nematic phase, *Biochemistry 27*, 428−436.
38. Lee, K. C., Hu, W., and Cross, T. A. (1993) 2H NMR determination of the global correlation time of the gramicidin channel in a lipid bilayer, *Biophys. J. 65*, 1162−1167.
39. Finer, E. G. (1973) Interpretation of deuterium nuclear magnetic resonance spectroscopic studies of the hydration of macromolecules, *J. Chem. Soc., Faraday Trans. 2 69*, 1590−1600.
40. Mendonca de Moraes, C., and Bechinger, B. (2004) Peptide-related alterations of membrane-associated water: Deuterium solid-state NMR investigations of phosphatidylcholine membranes at different hydration levels, *Magn. Reson. Chem. 42*, 155−161.
41. Volke, F., Eisenblatter, S., Galle, J., and Klose, G. (1994) Dynamic properties of water at phosphatidylcholine lipid-bilayer surfaces as seen by deuterium and pulsed field gradient proton NMR, *Chem. Phys. Lipids 70*, 121−131.
42. Prosser, R. S., Davis, J. H., Dahlquist, F. W., and Lindorfer, M. A. (1991) 2H nuclear magnetic resonance of the gramicidin a backbone in a phospholipid bilayer, *Biochemistry 30*, 4687−4696.
43. Prosser, R. S., Daleman, S. I., and Davis, J. H. (1994) The structure of an integral membrane peptide: a deuterium NMR study of gramicidin, *Biophys. J. 66*, 1415−1428.
44. Grobner, G., Burnett, I. J., Glaubitz, C., Choi, G., Mason, A. J., and Watts, A. (2000) Observations of light-induced structural changes of retinal within rhodopsin, *Nature 6788*, 810−813.
45. Van der Wel, P. C., Strandberg, E., Killian, J. A., and Koeppe, R. E. (2002) Geometry and intrinsic tilt of a tryptophan-anchored transmembrane alpha-helix determined by (2)H NMR, *Biophys. J. 83*, 1479−1488.
46. Glover, K. J., Whiles, J. A., Wood, M. J., Melacini, G., Komives, E. A., and Vold, R. R. (2001) Conformational dimorphism and transmembrane orientation of prion protein residues 110−136 in bicelles, *Biochemistry 40*, 13137−13142.
47. Whiles, J. A., Brasseur, R., Glover, K. J., Melacini, G., Komives, E. A., and Vold, R. R. (2001) Orientation and effects of mastoparan X on phospholipid bicelles, *Biophys. J. 80*, 280−293.
48. Whiles, J. A., Deems, R., Vold, R. R., and Dennis, E. A. (2002) Bicelles in structure−function studies of membrane-associated proteins, *Bioorg. Chem. 30*, 431−442.
49. Batchelder, L. S., Niu, H., and Torchia, D. A. (1983) Methyl reorientation in polycrystalline amino acids and peptides: A 2H NMR spin lattice relaxation study, *J. Am. Chem. Soc. 105*, 2228−2231.
50. Pines, A., Gibby, M. G., and Waugh, J. S. (1973) Proton-enhanced NMR of dilute spins in solids, *J. Chem. Phys. 59*, 569−590.
51. Abragam, A. (1961) *Principles of nuclear magnetism*, Oxford Scientific Publications, Oxford.
52. Davis, J. H. (1979) Deuterium magnetic resonance study of the gel and liquid crystalline phases of dipalmitoyl phosphatidylcholine, *Biophys. J. 27*, 339−358.

53. Davis, J. H., Jeffrey, K. R., Bloom, M., Valic, M. I., and Higgs, T. P. (1976) Quadrupolar echo deuteron magnetic resonance spectroscopy in ordered hydrocarbon chains, *Chem. Phys. Lett. 42*, 390−394.
54. Rance, M., and Byrd, R. A. (1983) Obtaining high-fidelity spin-1/2 powder spectra in anisotropic media: Phase-cycled Hahn Echo spectroscopy, *J. Magn. Reson. 52*, 221−240.
55. Bechinger, B., Aisenbrey, C., and Bertani, P. (2004) Topology, structure and dynamics of membrane-associated peptides by solid-state NMR spectroscopy, *Biochim. Biophys. Acta* (in press).
56. Harzer, U., and Bechinger, B. (2000) The alignment of lysine-anchored membrane peptides under conditions of hydrophobic mismatch: A CD, ^{15}N and ^{31}P solid-state NMR spectroscopy investigation, *Biochemistry 39*, 13106−13114.
57. Seelig, J. (1981) Deuterium and phosphorus nuclear magnetic resonance and fluorescence depolarization studies of functional reconstituted sacroplasmic reticulum membrane vesicles, *Biochemistry 20*, 3922−3932.
58. Matsuzaki, K., Murase, O., Tokuda, H., Funakoshi, S., Fujii, N., and Miyajima, K. (1994) Orientational and aggregational states of magainin 2 in phospholipid bilayers, *Biochemistry 33*, 3342−3349.
59. Ludtke, S., He, K., and Huang, H. (1995) Membrane thinning caused by magainin 2, *Biochemistry 34*, 16764−16769.
60. Münster, C., Spaar, A., Bechinger, B., and Salditt, T. (2002) Magainin2 in phospholipid bilayers: peptide orientation and lipid chanin ordering studied by X-ray diffraction, *Biochim. Biophys. Acta 1562*, 37−44.

BI049409H